DOI: 10.1002/adma.200602036

Two-Photon Excitation of Quantum-Dot-Based Fluorescence Resonance Energy Transfer and Its Applications**

By *Aaron R. Clapp*, *Thomas Pons*, *Igor L. Medintz*, *James B. Delehanty*, *Joseph S. Melinger*, *Theresa Tiefenbrunn*, *Philip E. Dawson*, *Brent R. Fisher*, *Brian O'Rourke*, and *Hedi Mattoussi**

Luminescent quantum dots (QDs), with their large absorption cross sections, superior photo- and chemical stability, broad excitation spectra, and narrow emission bandwidths, are excellent alternatives to traditional organic dyes for fluorescence labeling and emerging nanosensing applications.[1–10] Using various surface-functionalization techniques (including cap exchange and encapsulation methods), QDs can be dispersed in aqueous media.[3–5,10] This has naturally led to their use in biological applications, most notably in cellular labeling,[3,4,6,7,10] and in the development of sensitive assays that can detect small molecules and oligonucleotides in solution.[8,9] More recently, we and other groups have shown that QDs are unique donor fluorophores for fluorescence resonance energy transfer (FRET) where multiple acceptor dyes can be positioned around the QD to substantially enhance the overall rate of FRET between the QD and proximal dyes.[11–18] Because of its exquisite sensitivity to changes in donor–acceptor separation distance (with sixth power dependence), FRET has proven to be a powerful method for detecting molecular-scale interactions, such as binding events and changes in protein conformations. FRET-based QD–biomolecule sensing assemblies that are specific for the detection of target molecules including soluble 2,4,6-trinitrotoluene (TNT), DNA, and the activity of various proteolytic enzymes have been demonstrated.[14,19–21]

Multiphoton fluorescence microscopy is the preferred high-resolution imaging method for thick (ca. 1 mm) tissue samples owing to its intrinsic optical sectioning ability and limited out-of-focus photodamage. It also uses far red and near IR excitation (700–1100 nm), which is ideally located in the tissue optical transparency window.[22] However, FRET performance driven by two-photon excitation has been limited by the photophysical properties of organic dyes and fluorescent proteins. In particular, it is often difficult to devise a donor–acceptor pair with substantial spectral overlap for high FRET efficiency and nonoverlapping two-photon absorption spectra for limited acceptor direct excitation. A recent report by Larson et al. showed that water-soluble CdSe–ZnS QDs are superior probes for multiphoton fluorescence imaging where typical QD two-photon action cross sections are about one to two orders of magnitude larger than those of organic molecules designed specifically for such applications.[23]

In this report, we demonstrate efficient resonance energy transfer between luminescent QDs and proximal dye acceptors driven by a two-photon process using sub-band excitation energy (far red and near IR photoexcitation). The FRET process between QDs and proximal dyes using this format has two unique features: 1) it exploits the very high two-photon action cross sections of QDs compared to those of conventional dyes, which results in a near-zero background contribution from the dye acceptors due to direct excitation, independent of the excitation wavelength; 2) it provides high signal-to-background ratios in FRET imaging of cells and tissue samples by substantially reducing both autofluorescence and direct excitation contributions to the acceptor photoluminescence (PL) signal. These features can considerably simplify data analysis, in particular when signals of both the QD donor and dye acceptor are required to interpret assay results; they can also improve applications such as intracellular FRET sensing and imaging. Our findings also show that the energy transfer resulting from two-photon excitation is entirely con-

[*] Dr. H. Mattoussi, Dr. A. R. Clapp, Dr. T. Pons
Optical Sciences Division, Code 5611, US Naval Research Laboratory
Washington, DC 20375 (USA)
E-mail: hedi.mattoussi@nrl.navy.mil
Dr. I. L. Medintz, Dr. J. B. Delehanty
Center for Bio/Molecular Science and Engineering, Code 6900
US Naval Research Laboratory
Washington, DC 20375 (USA)
Dr. J. S. Melinger
Electronics Science and Technology Division, Code 6812
US Naval Research Laboratory
Washington, DC 20375 (USA)
T. Tiefenbrunn, Prof. P. E. Dawson
Departments of Cell Biology & Chemistry and
The Skaggs Institute for Chemical Biology, The Scripps Research Institute
La Jolla, CA 92037 (USA)
B. R. Fisher
Department of Chemistry, Massachusetts Institute of Technology
Cambridge, MA 02139 (USA)
Prof. B. O'Rourke
Institute of Molecular Cardiobiology
The Johns Hopkins University School of Medicine
Baltimore, MD 21205 (USA)

[**] This work was supported by grants from the Office of Naval Research (ONR), DARPA, and NIH. B.R.F., A.R.C., and T.P. were supported by fellowships from the Defense Science and Engineering Graduate Fellowship Program, the National Research Council, and la Fondation pour la Recherche Médicale (Paris), respectively. Supporting Information is available online from Wiley InterScience or from the authors.

ADVANCED MATERIALS

sistent with results collected using one-photon excitation (which uses higher energy photoexcitation), and in agreement with predictions of the Förster theory.

Table 1 shows the two-photon action cross-sectional values measured for our QDs in toluene and in water solutions, along with those of traditional dyes. Data show that the measured values for QDs are 2–3 orders of magnitude higher than Cyanine 3 (Cy3) or those reported in the literature for other common organic dyes.[24,25] Our measured values are comparable to the two-photon action cross sections reported in the literature.[23] Steady-state composite spectra collected from samples under two-photon excitation were deconvoluted to yield individual PL contributions using the known spectral profiles of isolated QDs and Cy3 dye emissions (see Fig. 1). In all cases, the PL contribution due to direct excitation was measured using control samples containing maltose binding protein (MBP)–Cy3 only and subtracted from the composite spectra before analysis. The QD PL spectra collected using a two-photon excitation mode maintain the same symmetric and narrow features as those collected in the one-photon excitation mode (compare Fig. 1A and C with Supporting Information Figs. S1 and S2 and the literature[13]). Time-resolved fluorescence measurements showed a pronounced decrease in QD donor lifetime for solutions of QD–MBP–Cy3 compared with unconjugated nanocrystals (see Fig. 1D and Fig. S3). The data also indicate that the Cy3 lifetime increases in the QD conjugate as compared to Cy3 alone. This observation is consistent with results using a one-photon excitation mode.[13,14] A decrease in QD steady-state PL and its lifetime were essentially negligible when QDs were mixed with free dye (control samples) due to negligible FRET interactions.

Table 1. Two-photon action cross sections for QDs populations in water and toluene, characterized using fluorescein as a standard in aqueous buffer ($\phi\sigma_{2P}$ = 36 GM at 800 nm and pH 13), Cy3, fluorescein and wild-type green fluorescent protein (GFP) (from the literature [28]). Although multiphoton absorption profiles are nonlinear optical phenomena, the longer wavelength emitting QD populations show higher two-photon action cross sections, consistent with the one-photon absorption behavior.

	Two-photon action cross section (GM, 800 nm)	
	water	toluene
510 nm QDs	8500	—
540 nm QDs	13800	15000
555 nm QDs	23200	19500
570 nm QDs	—	23000
Cy3	<1	—
Fluorescein	36	—
GFP	6	—

The results above indicate that the loss of QD emission is specifically due to self-assembly of the dye-labeled protein on the nanocrystal surface, which positions the dye acceptors close to the QD donor. This culminates in efficient nonradiative transfer of excitation energy from the QD to the proximal Cy3 dye (see Fig. 1). The experimental FRET efficiency can be readily determined using the relation (developed for one-photon excitation FRET):

$$E = 1 - \frac{F_{DA}}{F_D} \quad (1)$$

where F_{DA} and F_D are the QD PL measured in the presence and absence of dye acceptors, respectively.[26] Figure 1 shows that the FRET efficiency increases with the number of dyes, n, positioned near the QD surface. The data also show that the dependence of the FRET efficiency on the ratio n for the two-photon excitation mode is indistinguishable from the results using one-photon excitation (compare Fig. 1 and Supporting Information Figs. S1 and S2). The enhancement in the FRET efficiency with an increasing number of dyes is due to the increased effective overlap integral when multiple acceptors interact with a central QD donor.[13,14,26] However, the two-photon excitation mode essentially eliminated the undesired direct-excitation PL contribution common to the one-photon excitation case (compare the insets in Fig. 1C and Fig. S1). This is due to a vastly reduced two-photon absorption cross section (ca. 10^4 smaller) for the dye relative to QDs (see Table 1), indicating that the entire observed Cy3 signal from the QD–dye conjugates (collected by a charge-coupled device (CCD) detector) is attributed to nonradiative energy transfer. This is a desirable advantage over a one-photon mode where direct excitation of the acceptor, though generally small for an optimized excitation wavelength, must be carefully subtracted from the composite spectra to properly estimate the FRET efficiency. Analysis of the QD PL loss (or E) using Förster's formalism provided estimates of donor–acceptor distances r for both assemblies using the formula:

$$r = R_0 \left[\frac{n(1-E)}{E}\right]^{1/6} \quad (2)$$

where R_0 is the Förster distance.[13,26] The 510 nm QD–MBP–Cy3 and 540 nm QD–MBP–Cy3 titration results yielded fitted distances r of (67 ± 5) and (72 ± 4) Å, respectively, consistent with the known sizes of the QD bioconjugates and with values extracted using one-photon excitation mode.[13] Equivalence of the FRET processes using one- and two-photon excitation modes indicates that the transition dipole of the excited QD donor, which is responsible for nonradiative transfer of excitation energy, has the same properties regardless of the photoexcitation mechanism. Furthermore, the point dipole approximation is sufficient for describing QD fluorophores in this arrangement.[27]

We next demonstrate a unique advantage of two-photon excitation to probe energy transfer between QDs and conjugated dye acceptors, while investigating the stability of self-assembled QD–peptide conjugates within cells using fluorescence microscopy. Long-term stability of QD–protein conjugates is a crucial requirement in the design of QD-based intracellular sensors. 510 nm emitting QDs were conjugated with polyarginine-containing cell-penetrating peptides (CPPs) bearing an N-terminal polyhistidine tract, and subsequently incubated with human embryonic kidney (HEK 293T/17)

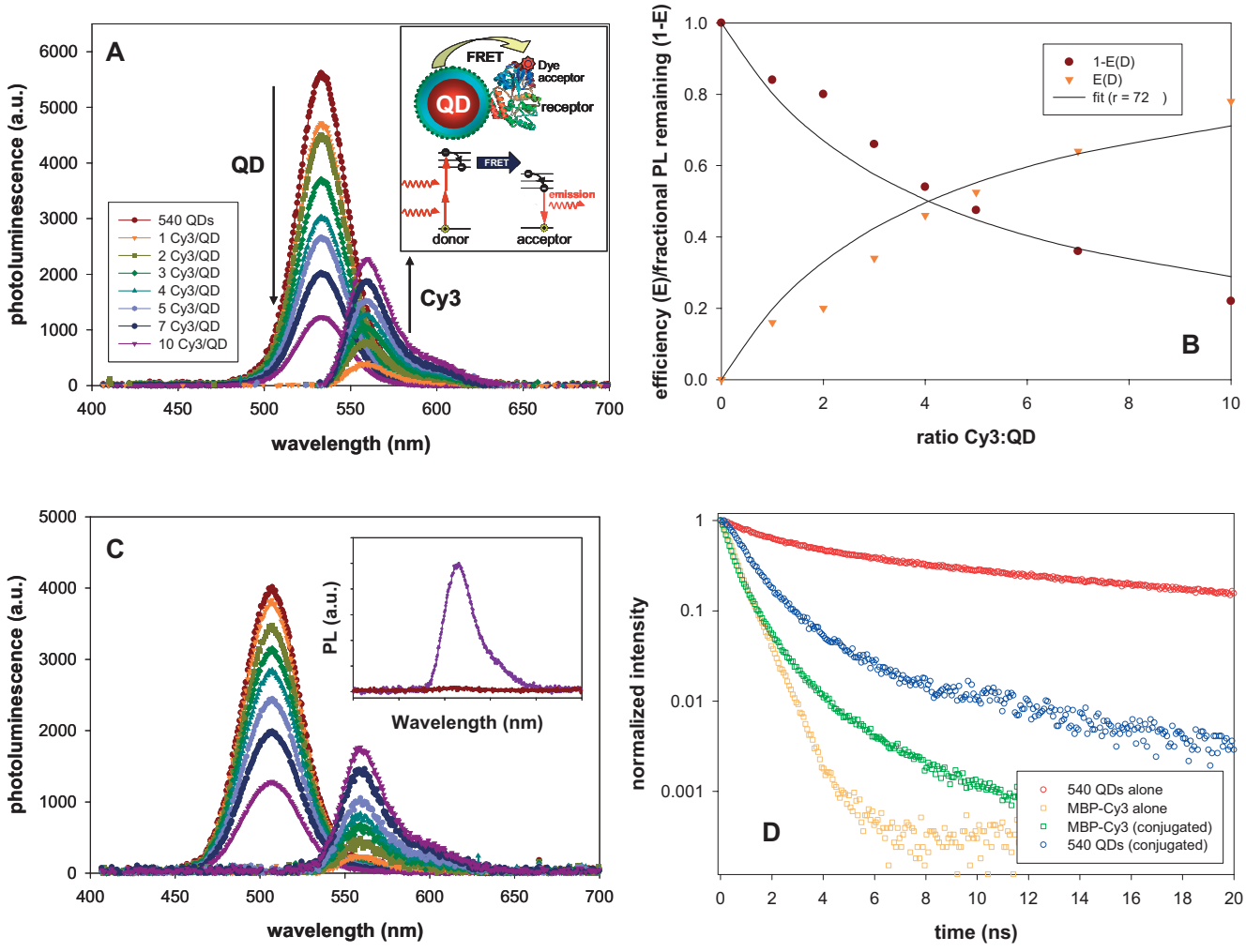

Figure 1. Deconvoluted PL spectra of QDs and Cy3 as a function of the number of MBP–Cy3 per QD using two-photon excitation, 540 nm QDs (A) and 510 nm QDs (C), along with the fractional PL (compared to unlabeled QD-conjugate solutions) and FRET efficiencies *E* for 540 nm QDs (B). The inset in (A) shows a schematic of a QD–protein–dye conjugate and FRET driven by a two-photon excitation process. The inset in (C) shows a comparison between FRET-induced Cy3 PL (purple) and the contribution due to direct two-photon excitation collected for a control MBP–Cy3 sample (crimson). D) Time-resolved fluorescence decays for 540 nm QD–MBP–Cy3 where the PL signals from donor and acceptor are spectrally isolated by appropriate band pass filters. Decay profiles are shown for isolated QDs, isolated MBP–Cy3, and for each fluorophore when brought together in a conjugate. Average lifetimes were estimated from fits of the experimental data to biexponential decays for all solutions [13]. Data from the Cy3 solution were well fit to a single-exponential decay function.

cells (assembled at a ratio of ca. 60 peptides per QD, 50 nM QD) for 1 h and fixed.[28] These peptides are known to mediate endocytosis of conjugated cargos such as proteins or nanoparticles in a wide variety of cell lines.[29,30] Two-photon excited fluorescence images of these cells revealed punctate QD staining consistent with endosomal uptake (Fig. 2A, top panels), which was notably absent when the cells were exposed to QDs alone, in agreement with our previous observations using this delivery mechanism reported in the literature.[28] When QDs were conjugated to both CPP and Cy3-labeled peptides (CPP–QD–peptide–Cy3, assembled at average ratios of 60 CPP and two Cy3-labeled peptides per QD), we observed efficient FRET from QDs to Cy3, as illustrated in Figure 2B (top panels). In contrast, staining of the cells with a mixture of Cy3-labeled transferrin (Tf–Cy3), a commonly used endosomal marker, and unlabeled CPP–QD does not show any evidence of Cy3 fluorescence (Fig. 2C, top panels). In the latter case, the dye was not directly conjugated to the QDs, thus preventing FRET interactions. We compared these two-photon fluorescence images with the corresponding one-photon epifluorescence images using 488 nm excitation (Fig. 2, bottom panels). While similar images were observed when cells were exposed to CPP–QD and CPP–QD–peptide–Cy3 conjugates, the cells showed bright Cy3 labeling upon exposure to a mixture of CPP–QD and Tf–Cy3 (compare Fig. 2C top panels and bottom panels). This demonstrates that significant Cy3 direct excitation occurred upon one-photon excitation at 488 nm (Fig. 2C, bottom panels). As a conse-

ADVANCED MATERIALS

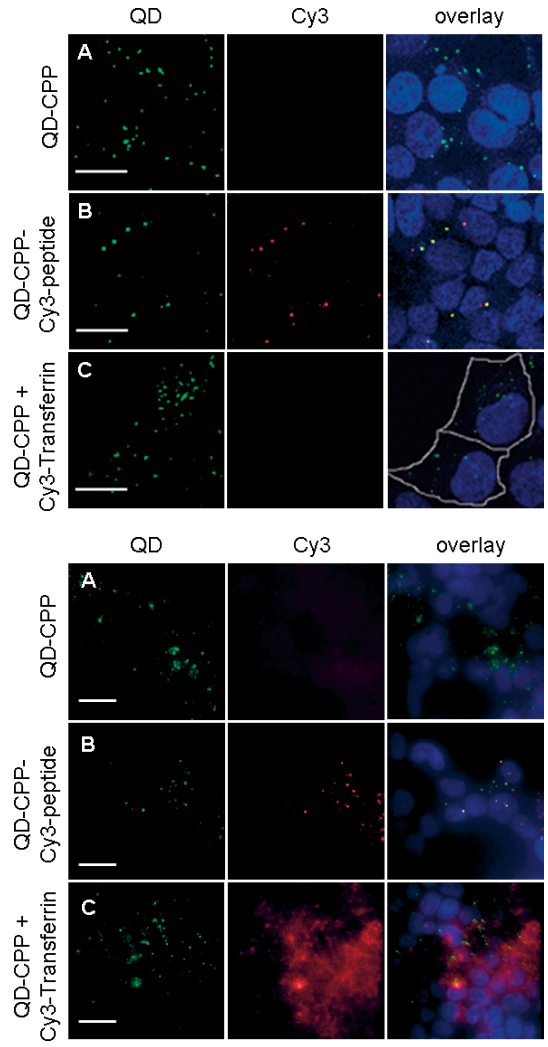

Figure 2. (top panels) Two-photon fluorescence microscopy images of HEK 293T/17 cells following incubation for 1 h with 510 nm QDs conjugated to: A,C) CPP and B) CPP and two Cy3-labeled peptides; CPP–QD conjugates were prepared with 60 CPP per QD. In (C), the cells were also incubated with Cy3 labeled-transferrin (not bound to QDs). The QD staining is located outside of the cell nuclei and within endosomal compartments as demonstrated by the overlaid image in (C); representative cell membranes are outlined in white. (λ_{ex} = 840 nm, scale bar = 20 μm). Rather high concentrations of DAPI nuclear stating agent (in comparison with QD and dye) were used to allow easy visualization of the cell nucleus in two-photon excitation mode. (bottom panels) One-photon fluorescence microscopy images of the same HEK 293T/17 cells corresponding to the conditions in A–C. The extremely weak fluorescence signal observed in panel A, middle image, is attributed to a slight leakage of the QD emission into the Cy3 window. (λ_{ex} = 488 nm, scale bar = 20 μm.)

quence, it is difficult to distinguish between Cy3 emission due to FRET and direct excitation in a one-photon mode, without additional background correction and image processing. Conversely, a PL signal due to the direct excitation of the acceptor dye was not observed in a two-photon excitation mode even at 20-fold molar excess relative to the QD donor. The absence of acceptor direct excitation contribution is a unique advantage of two-photon excited FRET using QD donors. While one-photon excitation was only able to probe the presence of QDs and Cy3, two-photon excitation unambiguously reveals colocalized fluorophores and efficient energy transfer from QDs to dyes when QD–peptide–dye conjugates are formed prior to endocytosis. Importantly, this has allowed us to demonstrate that the labeled peptides remained stably conjugated to QDs within the endosomal compartments after 72 h.

In the final example, we combined the unique features of two-photon excitation and FRET to implement a reagentless solution-phase sensing assembly specific for the nutrient sugar maltose. In this arrangement, a mutated form of MBP–His was labeled at the unique D41C residue such that binding to maltose induces a conformational transition (to a closed structure), which changes the local environment of the Cy3 dye and alters its fluorescence emission.[31] The FRET efficiency is not expected to change as the maltose concentration increases, but rather the PL of the acceptor will vary monotonically owing to changes in Cy3 quantum yield. Figure 3A shows the progression of steady-state fluorescence spectra with increasing maltose concentration. To account for slight variations in excitation efficiency between samples (due to fluctuations in laser power or other factors), we plotted the ratio between the Cy3 peak emission and that of the QD. Figure 3B shows these ratios as a function of maltose concentration using 510 and 540 nm emitting QDs in one and two-photon excitation modes. As the maltose concentration approaches the equilibrium dissociation constant, K_D, the Cy3 PL drops dramatically. A K_D of 0.8 mM was determined for this sensing assembly demonstrating that the response of the sensor is consistent irrespective of the QD population or the excitation method used.[31] In this sensing format, the QDs function primarily as light-harvesting fluorophores, effectively increasing the sensor two-photon cross section by several orders of magnitude and allowing its effective interrogation using two-photon excitation. (An alternate maltose sensing scheme was also evaluated using a two-photon excitation mode; see Supporting Information.)

In conclusion, multiphoton excitation of QDs presents several distinct advantages in fluorescence imaging that also extend to FRET-based applications using organic dyes as acceptors. Because of the very large two-photon action cross sections of luminescent CdSe–ZnS QDs as compared to dyes, direct excitation effects and spectral crosstalk can be reduced to background levels. As a result, detection of molecular-scale changes via FRET can be greatly simplified and improved using two-photon excitation. As nanosensing applications increasingly transition to intracellular environments, multiphoton excitation will allow more accurate targeting of structures and pathways. The interchangeable use of one and two-photon excitation processes in FRET-based sensing allows for the design and characterization of these tools prior to more complicated in vivo implementation. This generalized approach can be used to develop a wide range of unique sensing schemes for real-time intracellular detection, which are compatible with the benefits of multiphoton imaging techniques.

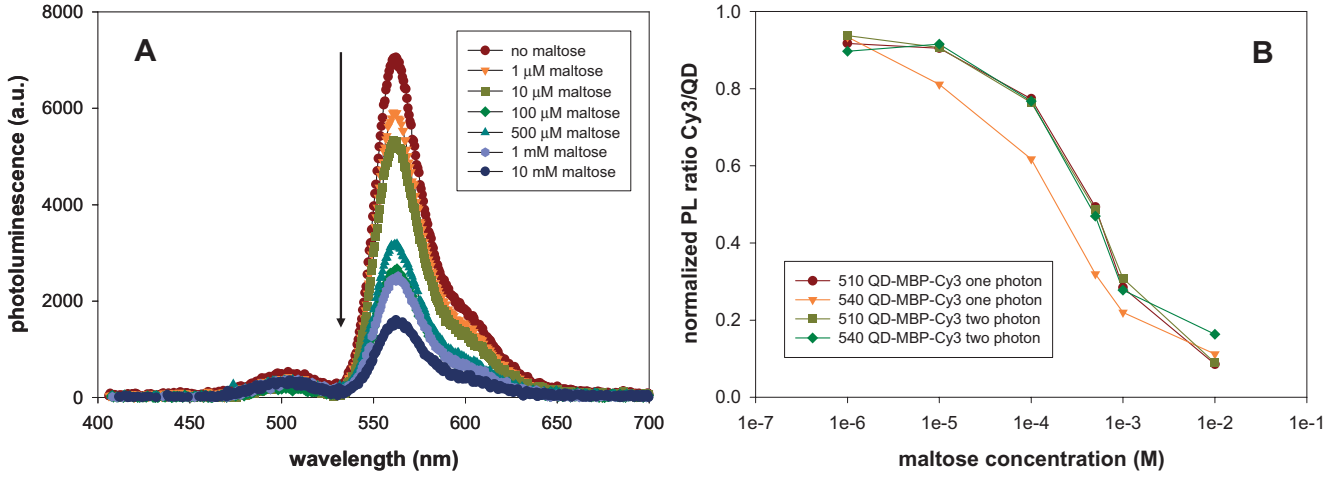

Figure 3. A) Composite spectra from a reagentless sensing format using 510 nm QDs with MBP–Cy3 labeled at Cys41. The Cy3 PL signal decreases monotonically as a function of maltose concentration. B) Transformation of the PL data versus maltose concentration for four different arrangements using 510 nm and 540 nm QDs with MBP–Cy3 using one- and two-photon excitation modes. The titration curves demonstrate the equivalence of the sensing arrangements regardless of the QDs used or excitation mode chosen.

Experimental

Quantum Dot–Protein Conjugates: Engineered variants of *E. coli* maltose binding protein were appended with a C-terminal polyhistidine tract (MBP–His) to allow metal-affinity-driven self-assembly on the surface of dihydrolipoic acid (DHLA)-functionalized QDs (see Supporting Information) [13,14]. These proteins were also modified to contain single cysteine mutations (at positions D41C or D95C) for specific labeling with maleimide-functionalized Cy3 dye prior to conjugate assembly. MBP–His labeled at D95C was used for the steady-state and time-resolved fluorescence experiments, while MBP–His labeled at D41C was exclusively used in the reagentless sensor design. The overall MBP/QD ratio was maintained at 15:1, thus ensuring essentially a complete coverage of the QD and maintaining a consistent QD quantum yield [13].

Quantum Dot–Peptide Conjugates: CPP was synthesized by Boc-solid phase peptide synthesis with the sequence $(His)_8$–Trp–Gly–Leu–Ala–Aib–Ser-Gly–$(Arg)_8$–amide, where Aib is the artificial residue alpha-amino isobutyric acid. The Cy3-labeled peptide was synthesized with the sequence, Ac–$(His)_6$–Gly–Leu–Aib–Ala–Ala–Gly–Gly–His–Tyr–Gly–Cys–NH_2, where Ac is an acetyl group at the N-terminus. This peptide was labeled with a maleimide-functionalized Cy3 (Amersham Biosciences, Piscataway, NJ) at the cysteine residue. The polyhistidine sequences at the N termini of the peptides allowed their self-assembly on the QD surface. QD conjugate stock solutions were prepared by incubating 1 μM of DHLA-capped QDs with the appropriate ratios of peptides, that is, 60 CPP/QD for CPP–QD conjugates, or 60 CPP mixed with two peptide–Cy3 per QD for CPP–QD–peptide–Cy3 conjugates.

Two-Photon Excited Steady-State Spectra: Two-photon excitation was generated using a tunable Ti–sapphire laser (200 fs pulse width, 76 MHz, Clark-MXR, Dexter, MI) operating at 800 nm and focused with an objective lens to a spot within a quartz cuvette containing the bioconjugates sample. Fluorescence spectra were collected using a spectrometer (SPEX 270M, HORIBA Jobin Yvon, Edison, NJ).

Fluorescence Lifetimes: The excitation source for the time-resolved experiments used the pulse-picked output (5 MHz) of a mode-locked Ti:Sapphire oscillator (pulse width < 200 fs, Mira 900, Coherent, Santa Clara, CA) with a center wavelength at 800 nm. PL was detected using an avalanche photodiode (SPCM-AQR-13, PerkinElmer, Wellesley, MA), and lifetimes were determined using a time correlated single-photon-counting system equipped with a TimeHarp 200 card and software (PicoQuant GmbH, Berlin, Germany).

Cell Imaging: Two-photon cell imaging was performed with a Bio-Rad MRC-1024MP confocal system (Bio-Rad, Hercules, CA) using ca. 10 mW of 840 nm pulsed excitation (ca. 80 fs, 80 MHz, Tsunami, Spectra-Physics, Mountain View, CA) at the focal plane of a 60×, 0.9 NA water immersion objective (E600FN upright microscope, Nikon, Melville, NY). DAPI, 510 nm QD, and Cy3 signals were separated using 490 and 550 nm dichroics. DAPI fluorescence crosstalk was subtracted from the QD channel. One-photon cell imaging of the same samples was performed with an Olympus IX71 inverted microscope and a Princeton Instruments I-PentaMAX CCD camera (Photometrics, Tucson, AZ). DAPI fluorescence was imaged using 350 nm excitation from a Xe lamp, while QDs and Cy3 were excited with a 488 nm Ar ion laser and spectrally separated using a 565 nm dichroic mirror.

Received: September 8, 2006
Revised: November 29, 2006
Published online: June 26, 2007

[1] X. Michalet, F. F. Pinaud, L. A. Bentolila, J. M. Tsay, S. Doose, J. J. Li, G. Sundaresan, A. M. Wu, S. S. Gambhir, S. Weiss, *Science* **2005**, *307*, 538.
[2] I. L. Medintz, H. T. Uyeda, E. R. Goldman, H. Mattoussi, *Nat. Mater.* **2005**, *4*, 435.
[3] M. Bruchez, M. Moronne, P. Gin, S. Weiss, A. P. Alivisatos, *Science* **1998**, *281*, 2013.
[4] W. Chan, S. Nie, *Science* **1998**, *281*, 2016.
[5] H. Mattoussi, J. M. Mauro, E. R. Goldman, G. P. Anderson, V. C. Sundar, F. V. Mikulec, M. G. Bawendi, *J. Am. Chem. Soc.* **2000**, *122*, 12 142.
[6] X. Wu, H. Liu, J. Liu, K. N. Haley, J. A. Treadway, J. P. Larson, N. Ge, F. Peale, M. P. Bruchez, *Nat. Biotechnol.* **2003**, *21*, 41.
[7] J. K. Jaiswal, H. Mattoussi, J. M. Mauro, S. M. Simon, *Nat. Biotechnol.* **2003**, *21*, 47.
[8] E. R. Goldman, G. P. Anderson, P. T. Tran, H. Mattoussi, P. T. Charles, J. M. Mauro, *Anal. Chem.* **2002**, *74*, 841.
[9] D. Gerion, W. J. Parak, S. C. Williams, D. Zanchet, C. M. Micheel, A. P. Alivisatos, *J. Am. Chem. Soc.* **2002**, *124*, 7070.

ADVANCED MATERIALS

[10] B. Dubertret, P. Skourides, D. J. Norris, V. Noireaux, A. H. Brivanlou, A. Libchaber, *Science* **2002**, *298*, 1759.
[11] P. T. Tran, E. R. Goldman, G. P. Anderson, J. M. Mauro, H. Mattoussi, *Phys. Status Solidi B* **2002**, *229*, 427.
[12] F. Patolsky, R. Gill, Y. Weizmann, T. Mokari, U. Banin, I. Willner, *J. Am. Chem. Soc.* **2003**, *125*, 13 918.
[13] A. R. Clapp, I. L. Medintz, J. M. Mauro, B. R. Fisher, M. G. Bawendi, H. Mattoussi, *J. Am. Chem. Soc.* **2004**, *126*, 301.
[14] I. L. Medintz, A. R. Clapp, H. Mattoussi, E. R. Goldman, J. M. Mauro, *Nat. Mater.* **2003**, *2*, 630.
[15] J. H. Kim, D. Morikis, M. Ozkan, *Sens. Actuators B* **2004**, *102*, 315.
[16] M. Levy, S. F. Cater, A. D. Ellington, *ChemBioChem* **2005**, *6*, 2163.
[17] T. Pons, I. L. Medintz, X. Wang, D. English, H. Mattoussi, *J. Am. Chem. Soc.* **2006**, *128*, 15 324.
[18] H. E. Grecco, K. A. Lidke, R. Heintzmann, D. S. Lidke, C. Spagnuolo, O. E. Martinez, E. A. Jares-Erijman, T. M. Jovin, *Microsc. Res. Tech.* **2004**, *65*, 169.
[19] E. R. Goldman, I. L. Medintz, J. L. Whitley, A. Hayhurst, A. R. Clapp, H. T. Uyeda, J. R. Deschamps, M. E. Lassman, H. Mattoussi, *J. Am. Chem. Soc.* **2005**, *127*, 6744.
[20] C.-Y. Zhang, H.-C. Yeh, M. T. Kuroki, T.-H. Wang, *Nat. Mater.* **2005**, *4*, 826.
[21] I. L. Medintz, A. R. Clapp, F. M. Brunel, T. Tiefenbrunn, H. T. Uyeda, E. L. Chang, J. R. Deschamps, P. E. Dawson, H. Mattoussi, *Nat. Mater.* **2006**, *5*, 581.
[22] W. Denk, J. H. Strickler, W. W. Webb, *Science* **1990**, *248*, 73.
[23] D. R. Larson, W. R. Zipfel, R. M. Williams, S. W. Clark, M. P. Bruchez, F. W. Wise, W. W. Webb, *Science* **2003**, *300*, 1434.
[24] M. A. Albota, C. Xu, W. W. Webb, *Appl. Opt.* **1998**, *37*, 7352.
[25] C. Xu, W. Zipfel, J. B. Shear, R. M. Williams, W. W. Webb, *Proc. Natl. Acad. Sci. USA* **1996**, *93*, 10 763.
[26] J. R. Lakowicz, *Principles of Fluorescence Spectroscopy*, 2nd ed. Kluwer, New York **1999**.
[27] A. R. Clapp, I. L. Medintz, H. Mattoussi, *ChemPhysChem* **2006**, *7*, 47.
[28] J. B. Delehanty, I. L. Medintz, T. Pons, P. E. Dawson, F. M. Brunel, H. Mattoussi, *Bioconjugate Chem.* **2006**, *17*, 920.
[29] S. Fawell, J. Seery, Y. Daikh, C. Moore, L. L. Chen, B. Pepinsky, J. Barsoum, *Proc. Natl. Acad. Sci. USA* **1994**, *91*, 664.
[30] L. Josephson, C. H. Tung, A. Moore, R. Weissleder, *Bioconjugate Chem.* **1999**, *10*, 186.
[31] I. L. Medintz, A. R. Clapp, J. S. Melinger, J. R. Deschamps, H. Mattoussi, *Adv. Mater.* **2005**, *17*, 2450.